

Delayed Recombination and Standard Rulers

Francesco De Bernardis¹, Rachel Bean², Silvia Galli^{1,5}, Alessandro Melchiorri¹, Joseph I. Silk³ and Licia Verde⁴

¹ *Universita' di Roma "La Sapienza", Ple Aldo Moro 2, 00185, Rome, Italy.*

² *Dept. of Astronomy, Space Sciences Building, Cornell University, Ithaca, NY 14853, USA.*

³ *Astrophysics, Denys Wilkinson Building, University of Oxford, Keble Road, OX1 3RH, Oxford, UK.*

⁴ *Institute of Space Sciences(IEEC-CSIC), Fac. Ciencies, Campus UAB, Bellaterra, Spain*

⁵ *Laboratoire Astroparticule et Cosmologie (APC),*

Universite' Paris Diderot - 75205 PARIS cedex 13.

Measurements of Baryonic Acoustic Oscillations in galaxy surveys have been recognized as a powerful tool for constraining dark energy. However, this method relies on the knowledge of the size of the acoustic horizon at recombination derived from Cosmic Microwave Background Anisotropy measurements. This estimate is typically derived assuming a standard recombination scheme; additional radiation sources can delay recombination altering the cosmic ionization history and the cosmological inferences drawn from CMB and BAO data. In this paper we quantify the effect of delayed recombination on the determination of dark energy parameters from future BAO surveys such as BOSS and WFMOS. We find the impact to be small but still not negligible. In particular, if recombination is non-standard (to a level still allowed by CMB data), but this is ignored, future surveys may incorrectly suggest the presence of a redshift dependent dark energy component. On the other hand, in the case of delayed recombination, adding to the analysis one extra parameter describing deviations from standard recombination, does not significantly degrade the error-bars on dark energy parameters and yields unbiased estimates. This is due to the CMB-BAO complementarity.

I. INTRODUCTION

A key goal of modern cosmology is to investigate the nature of the dark energy component, responsible for the current accelerated expansion of the Universe. A variety of observables, from Cosmic Microwave Background (CMB) anisotropies [1, 2] to galaxy surveys [3, 4, 5, 6, 7], will continue to be measured with increasingly refined accuracy in the next years thanks to a coordinated effort of satellite, ground based and balloon-borne missions. Despite the fact that it accounts for about 70% of the total energy density of the universe, dark energy is largely unclustered and is typically measured just by its effect on the evolution of the expansion history (i.e. the Hubble parameter) at redshift $z < 2$. Since the cosmic expansion depends on other key parameters as curvature or matter density, the nature of dark energy can therefore be revealed only by combination of different observables and/or observations over a wide redshift range.

A recent development in the field of large-scale galaxy surveys, is to use the measurement of Baryonic Acoustic Oscillations (BAO) [8, 9, 10] signal at $z < 2$ as a standard ruler. Oscillations in the primordial photon-baryon plasma leave an imprint in the matter distribution. Since the frequency of these oscillations is related to the size of the sound horizon at recombination, which is well constrained by CMB measurements, it is possible to use the measurements of those oscillations at different redshifts as a standard ruler and therefore determine the rate of the cosmic expansion.

It has been found that a number of theoretical systematics including non-linear growth, non-linear bias, and non-linear redshift distortions can be efficiently

modeled to minimize their contribution to uncertainties in the analysis of BAO observations [11, 12, 13]. As such, they are one of the key observables of the next decade in cosmology and it is therefore important to investigate how solid are the theoretical assumptions behind this method. A crucial assumption, indeed, is the possibility of having a very accurate measurement of the size of the acoustic horizon at recombination. [17] show that the interpretation of low redshift BAOs is robust if CMB correctly determines the baryon-to-photon ratio and the matter-radiation equality but not the matter baryon or photon densities alone. CMB measurements of these quantities is generally robust, but, in view of high-precision data, it is important to quantify any possible systematic effects introduced by deviations from the standard evolution of the early universe. Previous papers have studied, for example, the stability of the result under the hypothesis of an extra background of relativistic particles or early dark energy ([18]). In this case, the epoch of matter-photons equality is shifted and this may bias the determination of size the acoustic horizon if unaccounted for.

In this paper we consider another possible mechanism that could, in principle, affect the BAO interpretation as standard rulers if not modeled, namely a possible delay, or change in the recombination epoch that would result in a variation of the acoustic horizon. Several papers, recently, have indeed considered this hypothesis (see e.g. [14, 15, 16, 19, 20, 21, 22]). Dark matter decay or annihilation, black hole evaporation, or cosmic string decay can, for example, produce an extra background of resonance photons that could delay recombination (see [16] and references therein). More exotic mechanisms as, for example, variations

in the fine structure constant or in the Newton constant, can also lead to a modified recombination epoch ([23, 24]). We conclude that current constraints on delayed recombination are compatible with a change in the sound horizon which is non-negligible when compared with the precision for future BAOs data. This means that, if unaccounted for, delayed recombination could bias dark energy constraints from BAO. On the other hand, if delayed recombination is accounted for in the joint CMB-BAO analysis from forthcoming surveys, error-bars on dark energy parameters are only degraded by less than 10 % compared to the standard analysis.

The paper is organized as follows: in the next section we discuss delayed recombination and its effect on the sound horizon. In Sec. III we review the Fisher matrix formalism, while in Sec. IV we forecast the impact of delayed recombination on dark energy parameters inference for several future surveys. Finally, in Sec. IV, we draw together our findings and discuss the conclusions and their implications for future work.

II. DELAYED RECOMBINATION AND THE SOUND HORIZON

In this section we modify the standard recombination picture by including the possibility of extra sources of resonance (Lyman- α) photons. Note that we do not modify matter-radiation equality, an effect already explored by [17].

In the standard recombination scenario (see [25, 26]) the evolution of the electron ionization fraction, x_e is given by:

$$-\frac{dx_e}{dt} \Big|_{std} = C \left[a_c n x_e^2 - b_c (1 - x_e) \exp\left(-\frac{\Delta B}{k_B T}\right) \right] \quad (1)$$

where x_e is the electron fraction per hydrogen nuclei, n is the number density of atoms, a_c and b_c are the effective recombination and photo-ionization rates for principle quantum numbers ≥ 2 , ΔB is the difference in binding energy between the 1^{st} and 2^{nd} energy levels and

$$C = \frac{1 + K \Lambda_{1s2s} n_{1s}}{1 + K (\Lambda_{1s2s} + b_c) n_{1s}}, \quad K = \frac{\lambda_\alpha^3}{8\pi H(z)} \quad (2)$$

where λ_α is the wavelength of the single Ly- α transition from the $2p$ level, Λ_{1s2s} is the decay rate of the metastable $2s$ level, $n_{1s} = n(1 - x_e)$ is the number of neutral ground state H atoms, and $H(z)$ is the Hubble expansion factor at a redshift z .

As in [14, 15, 16], we include the possibility of extra resonance (Ly- α) photons at recombination with number density n_α which promote electrons to the $2p$ level (see [14, 19, 20, 21]):

$$\frac{dn_\alpha}{dt} = \varepsilon_\alpha H(z) n \quad (3)$$

where ε_α is assumed constant with redshift.

This leads to a modified evolution of the ionization fraction:

$$-\frac{dx_e}{dt} = -\frac{dx_e}{dt} \Big|_{std} - (1 - C) \varepsilon_\alpha H. \quad (4)$$

where std refers to the the standard scenario.

The introduction of ε_α has the main effect of delaying the redshift of recombination z_* . In the standard scenario this redshift is given by ([27]):

$$\begin{aligned} z_* &= 1048(1 + 0.00124\omega_b^{-0.738})(1 + g_1\omega_m^{g_2}) \quad (5) \\ g_1 &= 0.0783\omega_b^{-0.238}/(1 + 39.5\omega_b^{0.763}) \\ g_2 &= 0.560/(1 + 21.1\omega_b^{1.81}) \end{aligned}$$

where ω_m and ω_b are the matter and baryon physical energy densities respectively. Including positive values of ε_α decreases z_* as ([19]):

$$z_*(\varepsilon_\alpha) = (1 + 3\varepsilon_\alpha)^{-0.042} z_*(\varepsilon_\alpha = 0) \quad (6)$$

Conservative limits on ε_α from current CMB data are of the order of $\varepsilon_\alpha < 0.5$ at 95% c.l. ([16]). The redshift of recombination can therefore be smaller by $\sim 5\%$ respect to the standard case. These constraints were obtained for a Λ CDM cosmology: the bound on ε_α would be relaxed even further for models where dark energy is not a cosmological constant.

We can easily understand the main effect of a delayed recombination by looking at the variations in the visibility function which describes the density probability for last scattering for a photon at redshift z . Its peak defines therefore the epoch of recombination. As we can see from Figure 1, where we plot the visibility function defined as in [29] for different values of ε_α , an increase in ε_α shifts the visibility function towards lower redshifts and increases the width of the distribution. We can therefore expect two main effects on the CMB anisotropies: a displacement of the peaks in the anisotropy and polarization power spectra due to the shift in the recombination epoch and a simultaneous damping of the anisotropies (see Fig. 2) due to the increase in the finite thickness of the last scattering surface.

In what follows we quantify the impact of this effect on the acoustic oscillations imprinted in the matter power spectrum that can then be used as a ‘‘standard ruler’’ at lower redshifts. We investigate the variation of the sound horizon size s as a function of z_* and, therefore, ε_α . In fact galaxy surveys, by measuring the scale along and across the line of sight, constrain $H(z)^{-1}/s$ and $D_A(z)/s$, where D_A is the angular diameter distance at redshift z . It is therefore straightforward to expect that a systematic change in s could bias the determination of $H(z)^{-1}$, $D_A(z)$ and the derived parameters.

The size of the sound horizon s at recombination can be approximated by the following formula ([28]):

$$s = \frac{c}{\sqrt{3}H_0} \Omega_m^{-1/2} \int_0^{a_*} \frac{da}{\sqrt{(a + a_{\text{eq}})(1 + R(a))}}$$

$$\approx \frac{19.8 \text{ Mpc}}{\sqrt{\omega_b \omega_m}} \ln \left(\frac{\sqrt{R(a_*) + R(a_{\text{eq}})} + \sqrt{1 + R(a_*)}}{1 + \sqrt{R(a_{\text{eq}})}} \right)$$

where H_0 is the Hubble constant, a is the scale factor normalized to unity today, $R(a) = 30496\omega_b a$, the equality is at $a_{\text{eq}} = 1/(24185\omega_m)$ and $a_* = (1 + z_*)^{-1}$.

Shifting the epoch of recombination, while leaving as unchanged the remaining parameters, clearly changes the extrema of the integral and the size of the sound horizon.

In Figure 3 we show the percentage variation in s as a function of ϵ_α : a value of ϵ_α as large as 0.5 yields a few percent variation in the CMB estimate of the sound horizon. This can potentially propagate into a large shift in the recovered dark energy parameters: at $z \sim 0.6$ a $\sim 1\%$ error in s yields a $\sim 4\%$ error in w assumed constant. This shift is comparable to the statistical error on this quantity expected from forthcoming surveys. However, as we will see in the next sections and already from Figure 2, the impact of delayed recombination on observables is broader. Indeed, the damping in the anisotropy power spectrum introduces a degeneracy with other parameters as the scalar spectral index n_s . As showed in [16] considering values of $\epsilon_\alpha \sim 0.1$ could mimic variations as large as $\sim 10\%$ in n_s and in several other variables as the Hubble constant.

III. FISHER MATRIX ANALYSIS FOR BAO AND CMB: STANDARD RECOMBINATION

In this section we briefly review the Fisher formalism mostly based on the seminal paper by [30] and we

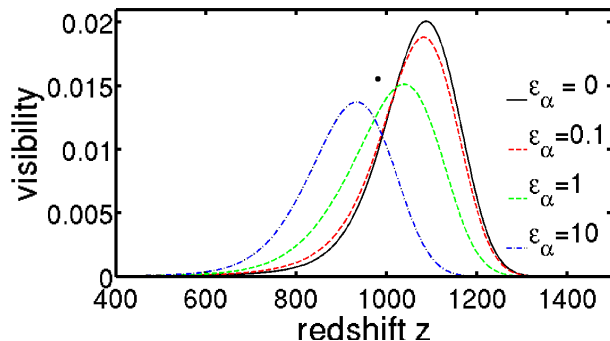


FIG. 1: Visibility function (defined as the density probability of photon last scattering), in function of ϵ_α . The inclusion of a delayed recombination shifts the peak of the distribution at lower redshift and increases its width.

refer the reader to this work for further clarifications. At the end of this section we cross-check our results with similar analyses already presented in the literature and obtained under the assumption of standard recombination.

The usual definition of the Fisher matrix is (see [31, 32]):

$$F_{\alpha\beta} \equiv \left\langle -\frac{\partial^2 \ln L}{\partial p_\alpha \partial p_\beta} \right\rangle \quad (8)$$

where L is the likelihood function for a set of parameters p_i . If we suppose that the likelihood has a maximum in some point of the parameter space p_i^0 , the fiducial model, and if the data have a normal distribution then the inverse of the Fisher matrix represents the covariance matrix of the parameters, i.e.:

$$\langle (p_\alpha - p_\alpha^0)(p_\beta - p_\beta^0) \rangle = (F^{-1})_{\alpha\beta}, \quad (9)$$

as a consequence the statistical errors on the parameters are given by the square root of the diagonal elements of the inverse Fisher matrix. According to the Cramer-Rao inequality ([33]) for unbiased estimators this is the best statistical error that one can obtain for the generic parameter p_α :

$$\sigma_{p_\alpha} \geq \sqrt{(F^{-1})_{\alpha\alpha}}. \quad (10)$$

For a galaxy survey the Fisher matrix can be approximated as ([34]):

$$F_{ij} = \int_{k_{\min}}^{k_{\max}} \frac{\partial \ln P(\vec{k})}{\partial p_i} \frac{\partial \ln P(\vec{k})}{\partial p_j} V_{\text{eff}}(\vec{k}) \frac{d\vec{k}}{2(2\pi)^3}$$

$$= \int_{-1}^1 \int_{k_{\min}}^{k_{\max}} \frac{\partial \ln P(k, \mu)}{\partial p_i} \frac{\partial \ln P(k, \mu)}{\partial p_j} V_{\text{eff}}(k, \mu) \frac{k^2}{8\pi^2} dk d\mu \quad (11)$$

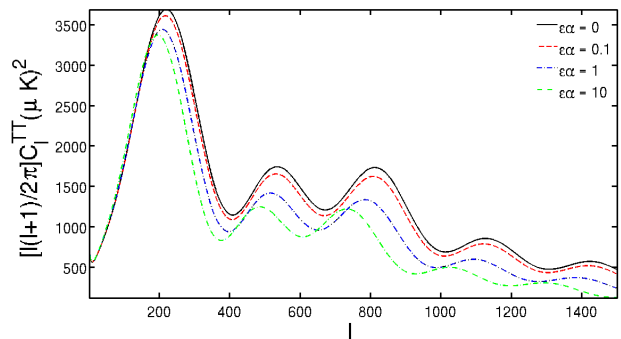


FIG. 2: Angular power spectrum of CMB anisotropies in function of ϵ_α . The inclusion of a delayed recombination shifts the peaks of the spectrum and damps the structure at small angular scales.

where the derivatives of the linear matter power spectrum $P(k, \mu)$ are evaluated at p_i^0 and V_{eff} is the effective volume of the survey, given by:

$$V_{eff}(k, \mu) = \int \left[\frac{n_g(\vec{r})P(k, \mu)}{n_g(\vec{r})P(k, \mu) + 1} \right]^2 d\vec{r} \quad (12)$$

$$= \left[\frac{n_g P(k, \mu)}{n_g P(k, \mu) + 1} \right]^2 V_{survey}$$

where in the last equality is assumed that the comoving number density of galaxies n_g is constant. The quantity μ is the cosine of the angle between the unit vector along the line of sight \hat{r} and the wave vector \vec{k} , $\mu = \vec{k} \cdot \hat{r}/k$. The integration over k that appears in (11) is performed only up to a k_{max} , to exclude non-linear scales. The value of k_{max} is redshift dependent and we calculate it using the same criterion of [30], i.e. requiring $\sigma(R) = 0.5$, where $R = \pi/2k$. The maximum scale of the survey, corresponding to k_{min} , doesn't influence the results and we can assume $k_{min} = 0$.

We consider two future surveys: the Baryon Oscillation Spectroscopic Survey (BOSS [35]), that will cover redshifts up to $z = 0.7$, and the Wide-Field Multi-Object Spectrograph (WF MOS [37]) splitted in two samples, the first (WF MOS1) at redshifts $0.5 < z < 1.3$ and the second (WF MOS2) covering $2.3 < z < 3.3$. We therefore divide the redshift space in six bins, one up to $z = 0.7$ for BOSS, four bins for WF MOS1 and one bin for WF MOS2. In Table I we list the survey area and the number of galaxies assumed in the analysis.

Following [30], we consider 6 cosmological parameters, the physical matter density $\Omega_m h^2$, the physical baryon density $\Omega_b h^2$, the matter fraction Ω_m , the optical depth to reionization τ , the scalar spectral index n_s and the normalization A_s . The fiducial model is given by $\Omega_m h^2 = 0.1274$, $\Omega_b h^2 = 0.021$, $\Omega_m = 0.26$, $\tau = 0.05$, $n_s = 0.96$, $A_s = 2.4 \cdot 10^{-9}$ and $h = 0.7$. We

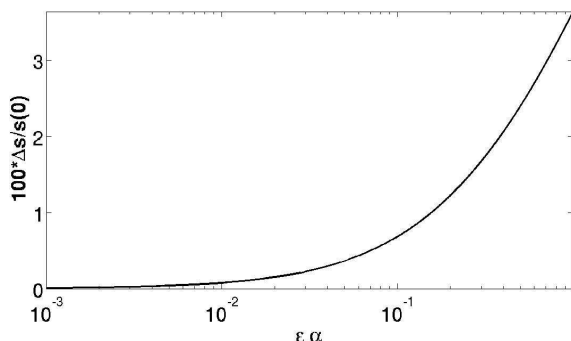


FIG. 3: Percentage of variation in the size of the acoustic horizon at recombination in function of ϵ_α . Delayed recombination with $\epsilon_\alpha \sim 0.5$ could increase the horizon by few percent.

Survey	z	$A(sq.deg.)$	$N(10^6)$
BOSS	< 0.7	8000	1.5
WF MOS1	$0.5 < z < 1.3$	2000	2.0
WF MOS2	$2.3 < z < 3.3$	300	0.6

TABLE I: Experimental specifications for the surveys used in this paper showing redshifts, survey area (A) and number of galaxies observed (N).

always assume flatness, i.e. $\Omega_\Lambda = 1 - \Omega_m$. In addition to these parameters we included other, redshift-dependent, parameters as the angular diameter distance $D_A(z)$, the Hubble parameter $H(z)$, the linear growth factor $G(z)$ and the linear redshift distortion $\beta(z)$. Our fiducial values for $H(z)$ and $D_A(z)$ are obtained assuming a cosmological constant model. For the bias we assume $b = 2$ at $z = 0.35$, $b = 3$ for WF MOS2 at $z = 2.8$ and values ranging from $b = 1.2$ at $z = 0.5$ to $b = 1.7$ for $z = 1.3$ for WF MOS1. With this parameterization each bin in redshift has a total of 10 parameters, 6 common to all bins and 4 different for each bin.

The observed power spectrum is given by:

$$P = \frac{D_{A,r}^2(z)H(z)}{D_A^2(z)H_r(z)} b^2 (1 + \beta\mu^2)^2 \left(\frac{G(z)}{G(0)} \right)^2 P^0(z=0, k) \quad (13)$$

where the first factor accounts for the fact that the observed cosmology (subscript r) could differ from the “true” cosmology, b is the bias, given by $b = \Omega_m(z)^{0.6}/\beta(z)$, and the term $(1 + \beta\mu^2)^2$ describes the linear redshift distortions. The linear growth factor $G(z)$ is given by the ratio $\delta(z)/\delta(0)$ between the linear density contrast at redshift z and at $z = 0$. We calculate the linear matter power spectrum at redshift $z = 0$, $P^0(z=0, k)$, using the numerical code CAMB [38]. For convenience we take the reference cosmology to be equal to our fiducial model.

The resulting Fisher matrix is combined with the CMB information from the Planck satellite [39]. For a CMB experiment the Fisher matrix is given by [36]:

$$F_{\alpha\beta}^{CMB} = \sum_{l=2}^{l_{max}} \sum_{i,j} \frac{\partial C_l^i}{\partial p_\alpha} (\text{Cov}_l)_{ij}^{-1} \frac{\partial C_l^j}{\partial p_\beta}, \quad (14)$$

where the C_l^{ij} are the well known power spectra for the temperature (TT), temperature-polarization (TE) and E-mode polarization (EE) (i and j run over TT, EE, TE) and Cov_l is the spectra covariance matrix.

We use the experimental configuration as described in Table II with $l_{max} = 1500$ to calculate the sum in (14). For the CMB Fisher matrix we include as a free parameter also the angular diameter distance to the last scattering surface $D_{A,CMB}$.

The full Fisher matrix is then simply given by the sum of the BAO Fisher matrices at each redshift bin

	Chan.	FWHM	$\Delta T/T$	$\Delta P/T$
$f_{\text{sky}} = 0.65$	70	14'	3.6	5.1
	100	9.5'	2.5	4.0
	143	7.1'	2.2	4.2
	217	5.0'	4.8	9.8

TABLE II: Experimental specifications for the Planck satellite. Channel frequency is given in GHz, FWHM in arcminutes, and noise in 10^{-6} .

Parameter	σ
$\Omega_m h^2$	0.0007
Ω_Λ	0.013
w_0	0.11
w_1	0.14

TABLE III: Uncertainties on dark energy and cosmological parameters from our Fisher matrix calculation in the case of standard recombination.

and the CMB:

$$F_{ij}^{\text{tot}} = F_{ij}^{\text{CMB}} + \sum_{z=1}^N F_{ij}^z \quad (15)$$

For N bins the total number of parameters is then $6 + N \times 4 + N_{\text{CMB}}$ where N_{CMB} is the number of additional parameters for the CMB, in this case $D_{A,\text{CMB}}$ (and hence $N_{\text{CMB}} = 1$). In the standard recombination case we have 6 bins in redshift and our full Fisher matrix has 31 parameters.

As explained in [30], by taking $D_A(z)$, $H(z)$ and $G(z)$ as separate parameters at each redshift one is avoiding any assumption about a specific dark energy model. The main advantage of this procedure is in considering a Fisher matrix which is independent on the dark energy model and that can be specified afterwards with a simple change of parameters. Here we allow for a possible time-dependent equation of state assuming a linear evolution with redshift:

$$w(z) = w_0 + w_1 z \quad (16)$$

To obtain constraints on dark energy we first select the set of parameters that affect distances and depend on dark energy, i.e. $\bar{p} = (\Omega_m h^2, \Omega_m, D_A(z)'s, H(z)'s)$ and we then marginalize over the remaining “nuisance” parameters. We implement this by inverting F_{ij}^{tot} and selecting from the inverted matrix the elements that correspond to the parameters of interest. We then invert this submatrix to obtain a Fisher matrix (F'_{nm}) just for $\Omega_m h^2, \Omega_m, D_A(z)'s$ and $H(z)'s$. Finally we project in a new parameter space, for example $\bar{q} = (\Omega_m h^2, \Omega_\Lambda, w_0, w_1)$, by equating the log likelihood functions in the old and in the new parameter space: $\ln L(\bar{p}) = \ln L(\bar{q})$. In the Fisher matrix

formalism this corresponds to a contraction of the old reduced Fisher matrix F'_{nm} with derivatives between old parameters and new parameters:

$$F_{ij}^{\text{new}} = \frac{\partial p_n}{\partial q_i} F'_{nm} \frac{\partial p_m}{\partial q_j} \quad (17)$$

The fiducial model is specified in the calculation of partial derivatives that appear in (17), we therefore assume a Λ -CDM model given by $w_0 = -1$ and $w_1 = 0$. The results from our Fisher matrix analysis for the dark energy parameters are shown in Table III. The results, obtained under the assumption of standard recombination, are substantially in agreement with those reported in [30], with errors on w_0 and w_1 of a factor ~ 2 smaller since we are considering improved experiments, with higher survey area and volumes. An improved Fisher matrix formalism has been recently presented in [12], based on numerical simulations of [40] and where nonlinear effects, bias and redshift distortions are more accurately implemented. The errors on D_A and H from their publicly available code for the BOSS survey at redshift $z = 0.35$ are respectively $\sim 1.1\%$ and $\sim 2.1\%$ to be compared with ours $\sigma_D/D \sim 1.5\%$ and $\sigma_H/H \sim 2\%$. We can therefore conclude that, for the scope of our paper, the results are in reasonable agreement.

Let us now describe in more detail the correlation between the different parameters in order to emphasize the importance of the CMB measurement of the sound horizon. In the BAO only Fisher matrix, strong correlations are present between the angular diameter distances $D_A(z)'s$ and $H(z)'s$ due to the poor determination of $\Omega_m h^2$, $\Omega_b h^2$ and n_s . These degeneracies can be reduced by an accurate CMB measurement of these cosmological parameters. As we can see from Table IV the correlations between the $D_A(z)'s$ and $H(z)'s$ (calculated as $\rho = (F^{-1})_{ij} / \sqrt{(F^{-1})_{ii}(F^{-1})_{jj}}$) from galaxy surveys alone are large, showing that, until the scale of sound horizon and other parameters are unknown, only the product $H(z)D_A(z)$ can be precisely determined from BAO surveys. It is clear from the above discussion that if the CMB information is biased by the assumption of an incorrect model of recombination, it will have an impact on the determination of the cosmic parameters from BAO. We investigate this in detail in the next section.

IV. DELAYED RECOMBINATION AND COSMOLOGICAL INFERENCES DRAWN FROM CMB AND BAO DATA

As shown in [41] it is easy to compute the shift in the best fit parameters when other parameters are fixed at a *wrong* fiducial value within the Fisher matrix formalism. In general if we fix a number p of parameters (say ψ_γ , with $\gamma = 1, \dots, p$) to an incorrect value which differs from the true value for an amount $\delta\psi_\gamma$, then

z	Surveys only			Surveys+CMB		
	$\sigma_D/D(\%)$	$\sigma_H/H(\%)$	ρ	$\sigma_D/D(\%)$	$\sigma_H/H(\%)$	ρ
0.35	8.39	8.48	-0.964	1.48	1.95	-0.151
0.6	8.57	8.82	-0.890	2.76	3.48	-0.160
0.8	8.16	8.27	-0.942	1.91	2.38	-0.157
1.0	8.10	8.17	-0.957	1.70	2.07	-0.212
1.2	8.01	8.06	-0.964	1.57	1.89	-0.225
2.8	7.93	7.24	-0.979	1.16	1.29	-0.217

TABLE IV: Relative uncertainties on $D_A(z)$'s and $H(z)$'s and their correlation coefficient (ρ) at each redshift. The correlation is large unless considering CMB observations, needed to calibrate the sound horizon.

the others n parameters (θ_α , with $\alpha = 1, \dots, n$) will be shifted of an amount given by:

$$\delta\theta_\alpha = -(F'^{-1})_{\alpha\beta} S_{\beta\gamma} \delta\psi_\gamma \quad \alpha, \beta = 1, \dots, n \quad (18)$$

where $(F'^{-1})_{\alpha\beta}$ is the inverse Fisher matrix in the space of θ_α parameters (an $n \times n$ matrix) and $S_{\beta\gamma}$ is a subset of the full $(n+p) \times (n+p)$ Fisher matrix including also the ψ_α parameters. Equation (18) shows that the shift on θ_α parameters depends on the correlations among various parameters, on how well these parameters are constrained and on how strong is the dependence of the observable from the p parameters fixed, i.e. on the derivatives of the observable with respect to the ψ_γ parameters, which are contained in the $S_{\beta\gamma}$ matrix. In our case we want to see what is the effect of assuming standard recombination, i.e. fixing $\epsilon_\alpha = 0$, while its true value is different from zero and we take it to be $\epsilon_\alpha = 0.05$.

To study the effects of a modified recombination on BAOs survey we follow the method described above computing first a Fisher matrix for the parameters listed in the previous section and then repeating the computation including also ϵ_α . We then select from this second Fisher matrix the sub-matrix $S_{\beta\gamma}$ that appear in (18), i.e. the row and the column corresponding to ϵ_α , and calculate the shift for the distances, Hubble parameters and dark energy parameters.

z	$\delta D/D$	$\delta H/H$
0.35	-3.0%	3.0%
0.6	-3.4%	3.3%
0.8	-3.6%	3.6%
1.0	-3.1%	3.0%
1.2	-3.4%	3.3%
2.8	-4.5%	4.5%

TABLE V: relative shift in the measure of $D_A(z)$ and $H(z)$ for the mean redshift of each bin as computed from (18) assuming $\epsilon_\alpha = 0$ in the hypothesis that true value is $\epsilon_\alpha = 0.05$.

We expect a shift δs in the value of sound horizon to cause a shift in angular diameter distances and Hubble parameters, being $D_A \propto s$ and $H \propto 1/s$. Moreover is easy to verify that relative shift in $D_A(z)$ and $H(z)$ at each redshift should be of the same extent and opposite: where $\delta D_A/D_A = -\delta H/H$. This is shown in Table V. Applying (18) to calculate shift in $D_A(z)$ and $H(z)$ confirms this, as shown in Table V. We show also absolute shifts in D_A and H for each bin in Figure 4. The shifts in D_A and H are at the 3%-4% level and, except for the last bin, are below the 95% C.L.

We remind that here we choose a fiducial model for the dark energy parameters with $w_0 = -1$ and $w_1 = 0$. Figure 5 shows that assuming an incorrect recombination model introduces a shift in the recovered value of w_0 towards $w_0 > -1$ and of w_1 towards negative values, as a consequence of the shifts on D_A and H . For $\Delta\epsilon_\alpha = 0.05$ the effect is comparable to the 1σ error on w_0 , and slightly larger for w_1 . With the incorrect recombination model, the best fit are shifted to $w_0 = -0.88$ and $w_1 = -0.22$ respect to the fiducial Λ -CDM model. An incorrect assumption on recombination could therefore mislead us towards claiming deviations of dark energy from a cosmological constant.

Even if this misinterpretation of the early universe physics induces shifts $< 95\%$ C.L. both for w_0 and w_1 , these results show that an incorrect calibration of sound horizon due to a wrong assumption for the recombination model could bias estimation of dark energy parameters by 10% or more.

As shown in Figure 5, to recover an unbiased best fit value for dark energy parameters (in our case the fiducial model, $w_0 = -1$ and $w_1 = 0$) the correct recombination model must be used and hence one has to introduce an additional parameter, ϵ_α in the analysis. Introducing this extra degree of freedom could in principle lead to an increase in the uncertainties on others parameters. We have verified that the increased uncertainty in the dark energy parameters is small. Including ϵ_α in the analysis increase 1σ errors on these parameters less than a 10% percent yield-

ing $\sigma_{w_0} = 0.12$ and $\sigma_{w_1} = 0.15$ (compare with III). Forthcoming data sets will thus disentangle effects of non-standard recombination from the effects of dark energy.

V. CONCLUSIONS

In this paper we have investigated how a biased determination of the sound horizon due to an incorrect recombination model affects cosmological parameters measurements from future BAO data. We have shown that assuming a standard recombination model when the true model is different can bias the measure of the CMB sound horizon and the best fit value of cosmological parameters such as the Hubble parameter. This shift propagates in a shift on the values of $D_A(z)$ and $H(z)$ and hence on the best fit values of w_0 and w_1 determined from BAO surveys. We have shown that a deviation from standard recombination which is still allowed by current CMB data, propagates in a bias in w_0 and w_1 comparable to their 1σ statistical error from forthcoming surveys. An incorrect calibration of sound horizon due to a wrong assumption for the recombination model could bias estimation of dark energy parameters by 10% or more. In this case future surveys may thus incorrectly suggest the presence of a redshift dependent dark energy component.

To recover an unbiased best fit value for dark energy parameters the correct recombination model must be

used or must be described by the set of cosmological parameters used in the analysis. We have concentrated on the case of delayed recombination where extra sources of resonance (Lyman- α) photons modify the evolution of the ionization fraction. This is well modeled by the addition of a single extra parameter. We have employed a Fisher matrix formalism to forecast errors and parameters biases for forthcoming CMB (Planck) and BAO (BOSS, WFMOS) surveys. For this data set combination, introducing the additional degree of freedom describing deviations from standard recombination does not significantly degrade the error-bars on dark energy parameters and yields unbiased estimates.

This is due to the CMB-BAO complementarity: forthcoming data sets will thus disentangle effects of non-standard recombination from the effects of dark energy.

VI. ACKNOWLEDGEMENTS

This research has been supported by ASI contract I/016/07/0 "COFIS". RB's work is supported by NASA ATP grant NNX08AH27G, NSF grants AST-0607018 and PHY-0555216 and Research Corporation. LV acknowledges the support of FP7-PEOPLE-2007- 4-3-IRG n 20218 and of CSIC I3 #200750I034.

-
- [1] G. Hinshaw *et al.* [WMAP Collaboration], arXiv:0803.0732 [astro-ph].
 - [2] E. Komatsu *et al.*, arXiv:0803.0547 [astro-ph].
 - [3] S. Cole *et al.* [The 2dFGRS Collaboration], Mon. Not. Roy. Astron. Soc. **362**, 505 (2005) [arXiv:astro-ph/0501174].
 - [4] M. Tegmark *et al.* [SDSS Collaboration], Phys. Rev. D **69**, 103501 (2004) [arXiv:astro-ph/0310723].
 - [5] M. Tegmark *et al.* [SDSS Collaboration], Phys. Rev. D **74**, 123507 (2006) [arXiv:astro-ph/0608632].
 - [6] M. Tegmark *et al.* [SDSS Collaboration], Astrophys. J. **606** (2004) 702 [arXiv:astro-ph/0310725].
 - [7] A. G. Sanchez *et al.*, Mon. Not. Roy. Astron. Soc. **366** (2006) 189 [arXiv:astro-ph/0507583].
 - [8] W. J. Percival *et al.*, Astrophys. J. **657**, 51 (2007) [arXiv:astro-ph/0608635].
 - [9] W. J. Percival, S. Cole, D. J. Eisenstein, R. C. Nichol, J. A. Peacock, A. C. Pope and A. S. Szalay, Mon. Not. Roy. Astron. Soc. **381**, 1053 (2007) [arXiv:0705.3323 [astro-ph]].
 - [10] D. J. Eisenstein *et al.* [SDSS Collaboration], "Detection of the Baryon Acoustic Peak in the Large-Scale Correlation Astrophys. J. **633**, 560 (2005) [arXiv:astro-ph/0501171].
 - [11] H. J. Seo, E. R. Siegel, D. J. Eisenstein and M. White, arXiv:0805.0117 [astro-ph].
 - [12] H. J. Seo and D. J. Eisenstein, arXiv:astro-ph/0701079.
 - [13] D. J. Eisenstein, H. j. Seo, E. Sirko and D. Spergel, Astrophys. J. **664**, 675 (2007) [arXiv:astro-ph/0604362].
 - [14] R. Bean, A. Melchiorri and J. Silk, Phys. Rev. D **68** (2003) 083501 [arXiv:astro-ph/0306357].
 - [15] R. Bean, A. Melchiorri and J. Silk, Phys. Rev. D **75** (2007) 063505 [arXiv:astro-ph/0701224].
 - [16] S. Galli, R. Bean, A. Melchiorri and J. Silk, arXiv:0807.1420 [astro-ph].
 - [17] D. J. Eisenstein and M. J. . White, Phys. Rev. D **70** (2004) 103523 [arXiv:astro-ph/0407539].
 - [18] E. V. Linder and G. Robbers, JCAP **0806**, 004 (2008) [arXiv:0803.2877 [astro-ph]].
 - [19] P.J.E. Peebles, S. Seager, W. Hu, *Astrophys. J.* **539** L1 (2000), astro-ph/0004389.
 - [20] P.D. Naselsky, I.D. Novikov *MNRAS* **334** 137 (2002), astro-ph/0112247
 - [21] A.G. Doroshkevich, I.P. Naselsky, P.D. Naselsky, I.D. Novikov, *Astrophys. J.* **586** 709 (2002), astro-ph/0208114.
 - [22] L. Zhang, X. L. Chen, Y. A. Lei and Z. G. Si, Phys. Rev. D **74**, 103519 (2006) [arXiv:astro-ph/0603425].
 - [23] S. Hannestad, *Phys. Rev. D* **60**, 023515 (1999); M. Kaplinghat, R. J. Scherrer & M S Turner, *Phys. Rev. D* **60**, 023516 (1999); P. P. Avelino *et al.*, PRD **62**, 123508 (2000); R. Battye, R. Crittenden & J. Weller, *Phys. Rev. D* **63**, 043505 (2001); P. P. Avelino *et al.*, *Phys. Rev. D* **64** (2001) 103505

- [arXiv:astro-ph/0102144] Landau, Harari & Zaldarriaga, *Phys. Rev. D* **63**, 083505 (2001). C. J. A. Martins, A. Melchiorri, G. Rocha, R. Trotta, P. P. Avelino and P. Viana, *Phys. Lett. B* **585**, 29 (2004) [arXiv:astro-ph/0302295]. G. Rocha, R. Trotta, C. J. A. Martins, A. Melchiorri, P. P. Avelino, R. Bean and P. T. P. Viana, *Mon. Not. Roy. Astron. Soc.* **352** (2004) 20 [arXiv:astro-ph/0309211]. C. J. A. Martins, A. Melchiorri, R. Trotta, R. Bean, G. Rocha, P. P. Avelino and P. T. P. Viana, *Phys. Rev. D* **66** (2002) 023505 [arXiv:astro-ph/0203149].
- [24] O. Zahn and M. Zaldarriaga, *Phys. Rev. D* **67** (2003) 063002 [arXiv:astro-ph/0212360].
- [25] P.J.E. Peebles, *Astrophys. J.* **153** 1 (1968).
- [26] Ya. B. Zel'dovich, V.G. Kurt, R.A. Sunyaev, *Zh. Eksp. Teoret. Fiz* **55** 278(1968), English translation, *Sov. Phys. JETP.* **28** 146 (1969).
- [27] Hu, W. & Sugiyama, N. 1996, *ApJ*, 471, 542
- [28] Efstathiou, G. & Bond J. R. 1999, *MNRAS*, 304, 75
- [29] U. Seljak and M. Zaldarriaga, *Astrophys. J.* **469** (1996) 437 [arXiv:astro-ph/9603033].
- [30] H. J. Seo and D. J. Eisenstein, *Astrophys. J.* **598** (2003) 720 [arXiv:astro-ph/0307460].
- [31] R. A. Fisher, *J. Roy. Stat. Soc.*, 98, 39 (1935)
- [32] M. Tegmark, A. N. Taylor, and A. F. Heavens, *ApJ* **480**, 22 (1997).
- [33] M. G. Kendall, A. Stuart, *The Advanced Theory of Statistics, Volume II* (Griffin, London, 1969).
- [34] M. Tegmark, *Phys. Rev. Lett.* **79** (1997) 3806 [arXiv:astro-ph/9706198].
- [35] www.sdss3.org
- [36] J. R. Bond, G. Efstathiou and M. Tegmark, *Mon. Not. Roy. Astron. Soc.* **291** (1997) L33 [arXiv:astro-ph/9702100].
- [37] K. Glazebrook, D. Eisenstein, A. Dey and B. Nichol, arXiv:astro-ph/0507457.
- [38] A. Lewis, A. Challinor, and A. Lasenby, *Astrophys. J.* **538**, 473 (2000), <http://camb.info>, astro-ph/9911177.
- [39] [Planck Collaboration], arXiv:astro-ph/0604069.
- [40] H. J. Seo and D. J. Eisenstein, *Astrophys. J.* **633** (2005) 575 [arXiv:astro-ph/0507338].
- [41] A. F. Heavens, T. D. Kitching and L. Verde, arXiv:astro-ph/0703191.

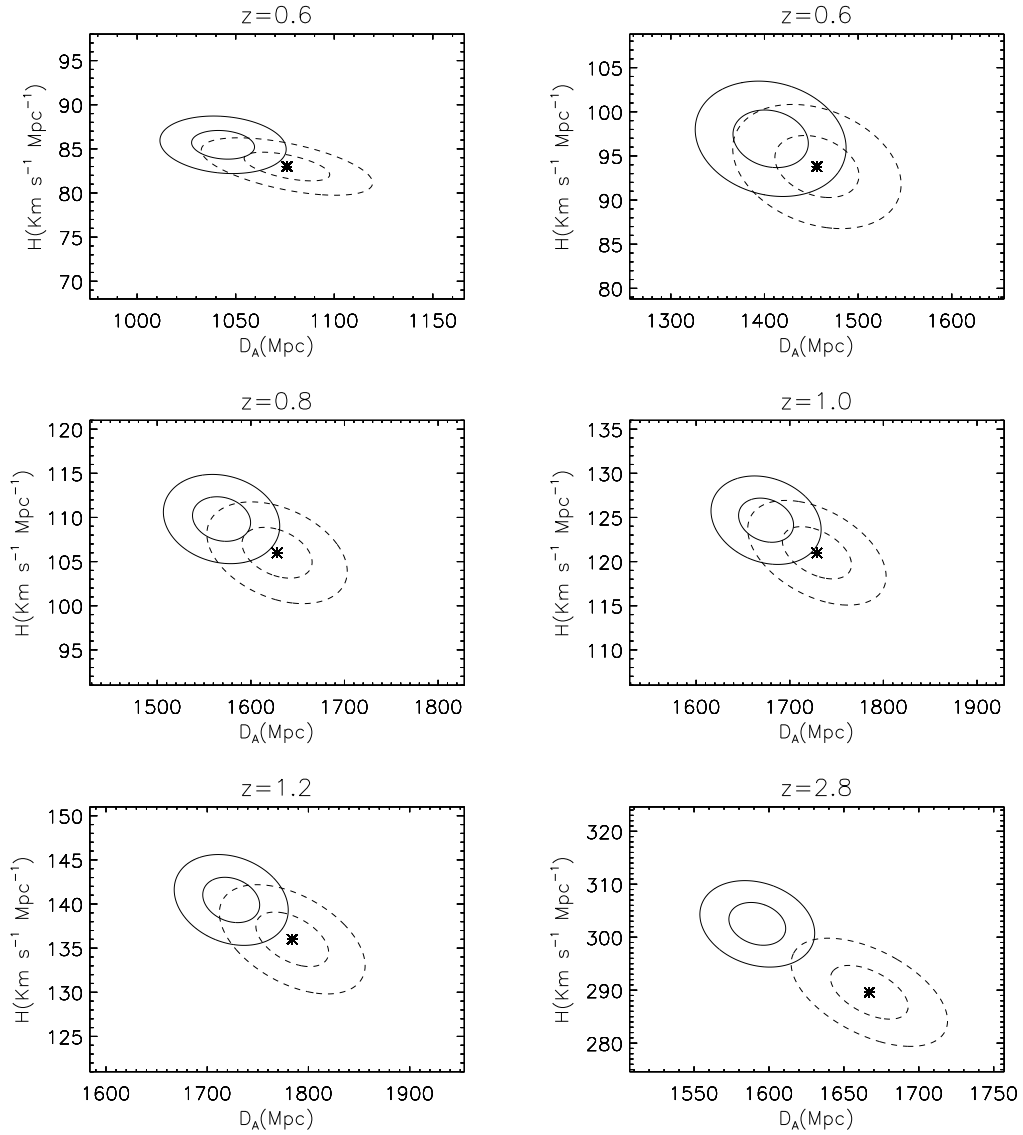


FIG. 4: Shifts on best fit of $D_A(z)$ and $H(z)$ (solid line) for the mean redshift of each bin caused by a wrong determination of sound horizon when fixing $\epsilon_\alpha = 0$ in the hypothesis that true value is $\epsilon_\alpha = 0.05$. Dashed contours are the $1,2 \sigma$ constraints obtained assuming the correct recombination model while solid contours assume standard recombination, The star is the correct fiducial model for $D_A(z)$ and $H(z)$.

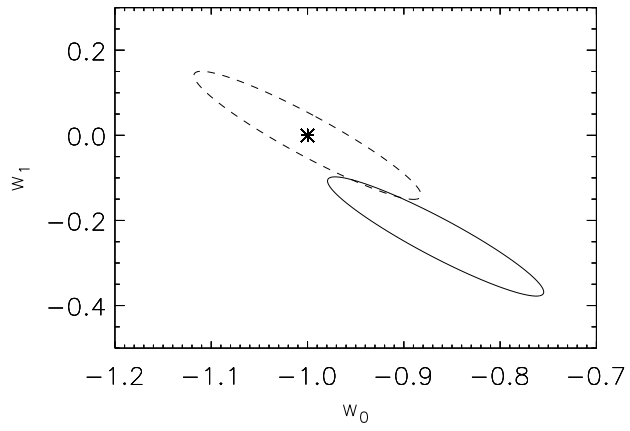


FIG. 5: Constraints at 68% c.l. on w_0 and w_1 , assuming an incorrect recombination model (solid line) and with the correct model (dashed line). The true model is indicated with the star.